

Organic magnetoresistance under resonant ac drive

R. C. Roundy and M. E. Raikh

Department of Physics and Astronomy, University of Utah, Salt Lake City, Utah 84112, USA

(Received 8 July 2013; revised manuscript received 5 August 2013; published 23 September 2013)

Motivated by a recent experiment, we develop a theory of organic magnetoresistance (OMAR) in the presence of a resonant ac drive. To this end, we perform a thorough analysis of the dynamics of ac-driven electron-hole polaron pair in magnetic field, which is a sum of external and random hyperfine fields. Resonant ac drive affects the OMAR by modifying the singlet content of the eigenmodes. This, in turn, leads to the change of recombination rate, and ultimately, to the change of the spin-blocking that controls the current. Our analysis demonstrates that, upon increasing the drive amplitude, the blocking eigenmodes of the triplet type acquire a singlet admixture and become unblocking. Most surprisingly, the opposite process goes in parallel: new blocking modes emerge from nonblocking precursors as the drive increases. These emergent blocking modes are similar to subradiant modes in the Dicke effect. A nontrivial evolution of eigenmodes translates into a nontrivial behavior of OMAR with the *amplitude* of the ac drive: it is initially linear, then passes through a maximum, drops, and finally saturates.

DOI: 10.1103/PhysRevB.88.125206

PACS number(s): 73.50.-h, 75.47.-m

I. INTRODUCTION

First papers reporting observation of spin injection into organic material (sexithienyl)¹ and spin-valve effect² with organic active layer (Alq₃) have launched a new field, organic spintronics, with numerous potential practical applications resulting from high tunability of organic-based structures. In the quest for fabrication of functional spin valves it was noticed that organic layers with nonmagnetized electrodes exhibit anomalous sensitivity to weak magnetic fields. This is how this sensitivity dubbed organic magnetoresistance (OMAR) became a subject of extensive experimental and theoretical studies.^{3–15} Until now, these studies were restricted to measurement of current change, $\delta I(B)$, and luminescence intensity change, $\delta I_L(B)$, with magnetic field, B , at different temperatures and applied voltages. However, $\delta I(B)$ and $\delta I_L(B)$ exhibit quite similar behaviors, and thus offer limited room for discriminating between different physical mechanisms. Partly because of this, a unique explanation and quantitative theory of OMAR is still debated. Meanwhile, there is a strong indication that the physics behind the OMAR phenomenon is fundamental. This is because the effect itself is robust, while its magnitude and even the sign are sensitive to technological details^{10–13} and intentionally imposed random fringe fields.¹⁶

The most “economic” theoretical description of OMAR so far was put forward in Ref. 8. It is appealing, in the sense that it relates OMAR to spin-blocking, which is its natural origin, in a most direct way by reducing it to the Larmor precession of spins within a *single* pair of carriers. The model of Ref. 8 was originally titled a “bipolaron model”; however, the basic physics of spin-selective processes that it captures is the same for either a bipolaron or an electron-hole pair. Still, to confirm or rule out the existing physical pictures of OMAR, it is desirable to supplement the measurements of $\delta I(B)$ and $\delta I_L(B)$ with probes of different aspects of OMAR. Viability of a certain OMAR model should be judged by how successfully it can account for results of these probes. One such probe was recently reported by Baker *et al.*¹⁷ They applied a transverse ac drive to organic-based diode, with bipolar injection, placed in magnetic field B_0 in which OMAR has practically saturated,

and observed a lively response in the form of a dip in $\delta I(B)$ at the resonance, $\omega_0 = \gamma B_0$, where γ is the gyromagnetic ratio. The dip got progressively deeper upon increasing the drive intensity.

In the present paper, we incorporate ac drive into the theory of OMAR and demonstrate that the two-site model⁸ offers very nontrivial predictions for the dependence of OMAR on the driving amplitude, B_1 , and on detuning of ω_0 from the resonance. In particular, we predict that the dependence $\delta I(B_1)$ is *nonmonotonic*. This behavior is a fingerprint of the ac-induced *trapping*, which we demonstrate. Experimental verification of this behavior would provide a strong support to the adequacy of the two-site model.

II. QUALITATIVE PICTURE

It is commonly accepted that, in organic materials, where the spin-orbit coupling is weak, spin-dependent phenomena are due to the random hyperfine fields with rms $b_0 \sim 10$ mT created by the nuclei. To relate OMAR to the spin dynamics of a single pair of polarons, it is sufficient to adopt the simplest assumption^{8,14,15} that bipolaron formation or recombination (in bipolar devices) proceed only when the pair-partners are in the singlet state, S . With equal probabilities of all initial states, the recombination time of a pair is determined by the hyperfine-field-induced admixture of the singlet to three other spin eigenstates.

It is a crucial ingredient of OMAR that the current response, $\delta I(B)$, at $B \sim b_0$ is governed by sparse *blocking* configurations⁸ in which hyperfine fields “conspire” to protect the pair from crossing into S after its creation. As the field increases and exceeds b_0 , these long-living states evolve into T_+ and T_- components of a triplet, and the current saturates.

From the perspective of blocking, the effect of ac drive on OMAR can be accounted for by considering the ac field as a mixing agent, which tends to scramble all three triplet states and, thus, to limit the trapping ability of T_+ , T_- ; see Fig. 1. In this way, the ac field tends to change the current toward its value at zero magnetic field, which is what was observed in Ref. 17. From the above picture one would expect that the

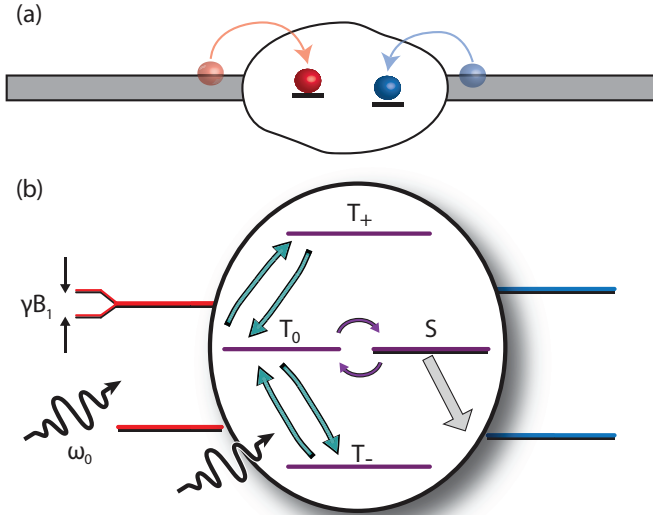


FIG. 1. (Color online) (a) Current passage through a bipolar device involves recombination of electron (red) and hole (blue) which occupy the neighboring sites; (b) Example of a pair in which electron is on-resonance and hole is off-resonance. The bubble illustrates the efficient mixing of the triplet components by the ac field, which, in turn, affects the crossing rate $T_0 \leftrightarrow S$. The gray arrow indicates that recombination occurs exclusively from S .

radiation-induced change of current, δI , is due to the change of the recombination rate, which, in turn, is proportional to B_1^2 , i.e., to the power of the driving field.

The main finding that we report is that the dependence of δI on B_1 is much more intricate. In particular, it is *linear* for weak B_1 . This effect stems from pairs in which one of the partners is on-resonance; see Fig. 1. It appears that for these particular pairs the radiation-induced suppression of trapping by T_+ and T_- is especially efficient. However, such pairs determine $\delta I(B_1)$ only for weak driving fields, namely, for fields in which the nutation frequency is much smaller than γb_0 . As we will proceed to show, a very nontrivial physics unfolds for higher B_1 . Quite unexpectedly, a new *long-living mode*, $\frac{1}{\sqrt{2}}(T_+ - T_-)$, emerges in strong enough driving fields; see Fig. 2. This mode, in which both pair-partners are on resonance, is fully analogous to subradiant state in the Dicke effect.¹⁸ In this regard, we would like to note that although the Dicke physics for an ensemble of atoms in an excited state has been known for almost 60 years, the fact that it can emerge as a result of ac drive has never been considered before. Trapping by this “subradiant” state also yields a linear correction to the current, but with *opposite slope*.

III. DRIVEN SPIN-PAIR WITHOUT RECOMBINATION

To highlight the physics, we first neglect recombination. Since the experiment in Ref. 17 was performed on a bipolar device, we start with the Hamiltonian of a driven electron-hole pair,

$$\hat{H} = \omega_e S_e^z + \omega_h S_h^z + 2\Omega_R (S_e^x + S_h^x) \cos \omega_0 t, \quad (1)$$

where $\omega_{e,h} = \omega_0 + \delta_{e,h}$, $\Omega_R = \gamma B_1$ is the Rabi frequency, and $\delta_{e,h}$ are the z components of the hyperfine fields acting

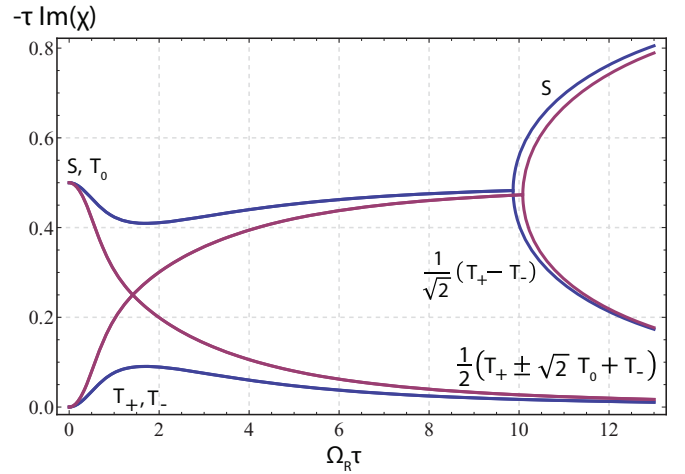


FIG. 2. (Color online) The evolution of dimensionless decay rates of different modes with amplitude of the ac drive is plotted from Eq. (10) for two sets of parameters $(\delta\tau, \delta_0\tau)$: blue (2.5,2); purple (2,2.5). The content of the quasimodes evolves from T_+, T_- and linear combinations of S, T_0 at weak drive into the combinations, $\frac{1}{2}(T_+ \pm \sqrt{2}T_0 + T_-)$, one superradiant mode, S , and one subradiant mode, $\frac{1}{\sqrt{2}}(T_+ - T_-)$.

on the electron and hole, respectively, i.e., the detunings of the pair-partners from the resonance. By retaining only z components, we assumed that $B_0 \gg b_0$. We will also assume that $\gamma B_0 \gg \Omega_R$, which allows us to employ the rotating wave approximation. In the rotating frame, the amplitudes of T_+, T_-, T_0 , and S components of the wave function are related by a system,

$$(\chi - \delta)A_{T_-} = \frac{\Omega_R}{\sqrt{2}}A_{T_0}, \quad (2)$$

$$(\chi + \delta)A_{T_+} = \frac{\Omega_R}{\sqrt{2}}A_{T_0}, \quad (3)$$

$$\chi A_S = -\delta_0 A_{T_0}, \quad (4)$$

$$\chi A_{T_0} = -\delta_0 A_S + \frac{\Omega_R}{\sqrt{2}}(A_{T_+} + A_{T_-}), \quad (5)$$

where χ is the quasienergy (see Fig. 3), while parameters δ_0 and δ are defined as

$$\delta_0 = \frac{1}{2}(\delta_e - \delta_h), \quad \delta = \frac{1}{2}(\delta_e + \delta_h). \quad (6)$$

The quasienergies satisfy the equation

$$\chi^2(\chi^2 - \delta^2 - \Omega_R^2) - \delta_0^2(\chi^2 - \delta^2) = 0, \quad (7)$$

with obvious solutions

$$\chi = \pm \frac{1}{2}[(\delta_0 + \delta)^2 + \Omega_R^2]^{1/2} \pm \frac{1}{2}[(\delta_0 - \delta)^2 + \Omega_R^2]^{1/2}. \quad (8)$$

It follows from Eqs. (2) and (7) that for large $\Omega_R \gg \delta_0, \delta$, the pair of quasienergies, which approaches $\chi = 0$ (see Fig. 3), corresponds to the modes S and $\frac{1}{\sqrt{2}}(T_+ - T_-)$, while the quasienergies that approach $\chi = \pm\Omega_R$ correspond to the combinations $\frac{1}{2}(T_+ \pm \sqrt{2}T_0 + T_-)$, respectively.

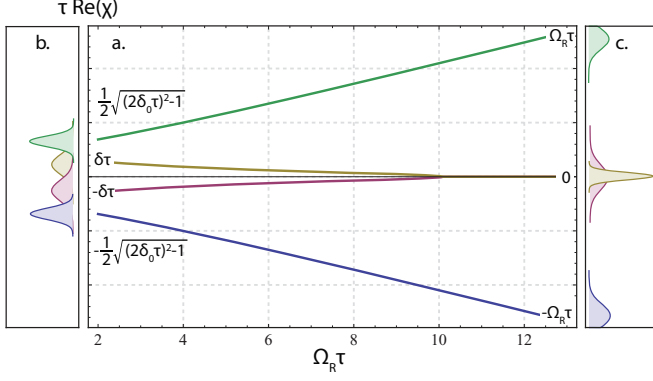


FIG. 3. (Color online) (a) The evolution of quasienergies with amplitude of the driving field is plotted from Eq. (10) for parameters $(\delta\tau, \delta_0\tau) = (2, 2.5)$. Quasienergies evolve from $\pm\delta, \pm\frac{1}{2}\sqrt{(2\delta_0\tau)^2 - 1}$ to $0, \pm\Omega_R\tau$. At small Ω_R , the quasienergies are well resolved (b). Merging of two quasienergies at large Ω_R is accompanied by splitting of their widths (c), which is a manifestation of the Dicke physics.

IV. DRIVEN SPIN-PAIR WITH RECOMBINATION

Including recombination from S requires the analysis of the full equation for the density matrix,

$$i\dot{\rho} = [\hat{H}, \rho] - \frac{i}{2\tau}\{\Pi_S, \rho\}, \quad (9)$$

where τ is the recombination time, and Π_S is the projector onto the singlet subspace. The matrix corresponding to this equation is 16×16 . The 16 eigenvalues can be cast in the form $\chi_i - \chi_j^*$, where χ_i and χ_j satisfy the quartic equation

$$\chi \left(\chi + \frac{i}{\tau} \right) (\chi^2 - \delta^2 - \Omega_R^2) - \delta_0^2 (\chi^2 - \delta^2) = 0, \quad (10)$$

which generalizes Eq. (7) to the pair with decay. For slow recombination, $b_0\tau \gg 1$, the quasienergies acquire small imaginary parts, which can be found perturbatively from Eq. (10):

$$\delta\chi = -\frac{i}{4\tau} \left(1 \pm \frac{|\delta_0^2 - \delta^2 - \Omega_R^2|}{\sqrt{(\delta^2 + \delta_0^2 + \Omega_R^2)^2 - 4\delta_0^2\delta^2}} \right). \quad (11)$$

Naturally, in the limit $\Omega_R \rightarrow 0$, Eq. (11) yields either $\delta\chi = -i/2\tau$ for S and T_0 states, and $\delta\chi = 0$ for the trapping states T_+ and T_- . Less trivial is that at large $\Omega_R \gg \delta_0, \delta$, the values $\delta\chi$ again approach $\delta\chi = -i/2\tau$ and $\delta\chi = 0$. The evolution of the imaginary parts of the quasienergies with Ω_R is illustrated in Fig. 2.

V. CURRENT AT A WEAK DRIVE

Finite $\Omega_R \ll \delta, \delta_0 \sim b_0$ leads to finite lifetimes of the trapping modes. Expanding Eq. (11), we get

$$\tau_{\text{tr}} = \frac{1}{2|\chi|} = \frac{4\tau(\delta^2 - \delta_0^2)^2}{\Omega_R^2\delta_0^2}. \quad (12)$$

Once τ_{tr} is known, we can employ the simplest quantitative description of transport¹⁵ based on the model Ref. 8 to express the correction, $\delta I(\Omega_R)$, to the current caused by the ac drive. Within this description, a pair at a given site is first assembled,

then undergoes the pair-dynamics and either recombines or gets disassembled depending on which process takes less time; see Fig. 1 (a). These three steps are then repeated, so that the passage of current proceeds in cycles. Then the current associated with a given pair is equal to $\frac{1}{\langle t \rangle}$, where $\langle t \rangle$ is the average cycle duration. Importantly, all the initial spin configurations of the pair have equal probabilities. For simplicity, it is assumed¹⁵ that, on average, the times of assembly and disassembly are the same $\tau_D \gg \tau$. This input is sufficient to derive the following expression for $\delta I(\Omega_R)$

$$\frac{\delta I(\Omega_R)}{I(0)} = \frac{\tau_{\text{tr}}^{-1}}{\tau_{\text{tr}}^{-1} + 2\tau_D^{-1}} = \frac{\Omega_R^2\delta_0^2}{\Omega_R^2\delta_0^2 + 8(\delta^2 - \delta_0^2)^2 \frac{\tau}{\tau_D}}, \quad (13)$$

where $I(0) = \frac{1}{\tau_D}$. The remaining task is to average Eq. (13) over the distributions of the hyperfine fields, or equivalently, over δ and δ_0 . Since we consider a weak drive, this averaging is greatly simplified. Indeed, the major contributions to the average comes from narrow domains $|\delta - \delta_0| \sim \Omega_R(\frac{\tau_D}{\tau})^{1/2}$ and $|\delta + \delta_0| \sim \Omega_R(\frac{\tau_D}{\tau})^{1/2}$, much narrower than b_0 . On the other hand, these domains are wider than Ω_R , which justifies the expansion Eq. (12). Replacing the distribution functions of $(\delta + \delta_0)$ and $(\delta - \delta_0)$ by $\frac{1}{\sqrt{\pi}b_0}$, we get

$$\begin{aligned} \frac{\langle \delta I(\Omega_R) \rangle}{I(0)} &= \frac{\Omega_R^2}{(2\pi)^{1/2}b_0} \int \frac{d(\delta - \delta_0)}{\Omega_R^2 + \frac{32\tau}{\tau_D}(\delta - \delta_0)^2} \\ &+ \frac{\Omega_R^2}{(2\pi)^{1/2}b_0} \int \frac{d(\delta + \delta_0)}{\Omega_R^2 + \frac{32\tau}{\tau_D}(\delta + \delta_0)^2} \\ &= \left(\frac{\pi\tau_D}{2\tau} \right)^{1/2} \left(\frac{\Omega_R}{b_0} \right), \end{aligned} \quad (14)$$

i.e., the radiation-induced correction is *linear* in Ω_R . To understand this anomalous behavior qualitatively, notice that small $(\delta + \delta_0)$ and $(\delta - \delta_0)$ correspond to small δ_e and δ_h , respectively. Therefore, the linear $\delta I(\Omega_R)$ comes from configurations of hyperfine fields in which one of the pair-partners is on-resonance,^{19–21} this partner responds strongly to the ac drive. The ratio Ω_R/b_0 is the portion of such configurations. The upper boundary of the weak driving domain is set by the condition $\Omega_R\sqrt{\tau_D/\tau} \lesssim b_0$, which allowed us to replace the distribution functions of $\delta - \delta_0, \delta + \delta_0$ by a constant. It is also seen from Eq. (13) that for $\Omega_R \gg b_0\sqrt{\tau_D/\tau}$ that the correction saturates at $\langle \delta I \rangle / I(0) = 1$. This saturation applies as long as T_+ and T_- are the trapping eigenmodes. As was mentioned above, upon increasing Ω_R , the trapping eigenmodes evolve into $\frac{1}{2}(T_+ \pm \sqrt{2}T_0 + T_-)$ and we enter the strong-driving regime.

VI. STRONG DRIVE

Expanding Eq. (11) in the limit $\Omega_R \gg \delta, \delta_0$ yields the expression $\tau_{\text{tr}} \approx \tau\Omega_R^2/\delta_0^2$ for the lifetime of the trapping eigenmodes. The same steps that led to Eq. (13) give rise to the following *negative* correction to the current:

$$\frac{\delta I(\Omega_R)}{I(0)} = 1 - \left(\frac{\tau}{\tau_D} \right) \frac{\Omega_R^2}{\delta_0^2 + \frac{\tau}{\tau_D}\Omega_R^2}. \quad (16)$$

We see from Eq. (16) that at $\Omega_R \gg (\frac{\tau_D}{\tau})^{1/2}b_0$ the current is the same as it was in the absence of the ac drive. This is

due to the fact that both in the absence of drive and in this domain the number of long-living modes is two. The return of $\delta I(\Omega_R)$ to zero takes place over a parametrically broad interval $\sqrt{\frac{\tau}{\tau_D}} < \frac{\Omega_R}{b_0} < \sqrt{\frac{\tau_D}{\tau}}$. The slope is calculated upon averaging Eq. (16) over δ_0 , which again can be carried out after replacing the distribution function by $\frac{1}{\sqrt{\pi}b_0}$ and yields

$$\frac{1}{I(0)} \frac{\partial \langle \delta I \rangle}{\partial \Omega_R} = - \left(\frac{\tau}{\pi \tau_D} \right)^{1/2} \frac{1}{b_0}. \quad (17)$$

We see that the strong-field slope is τ_D/τ times smaller than the weak-field slope given by Eq. (14); this is consistent with the fact that the domain of the current drop is τ_D/τ times broader than the domain of current growth.

In fact, the saturation predicted by Eq. (16) precedes another domain of change of current, which stems from bifurcation in lifetimes of S, T_0 modes at large Ω_R ; see Fig 2. To capture this bifurcation analytically, notice that for large Ω_R Eq. (11) predicts for $\delta\chi = -\frac{i}{2\tau}$ for the $\frac{1}{\sqrt{2}}(T_+ - T_-)$ -mode, while the zero-order value of quasienergy falls off with Ω_R as $\delta_0\delta/\Omega_R$. Therefore, when Ω_R exceeds $\delta\delta_0\tau$, the correction would exceed the zero-order value and the perturbative treatment becomes inapplicable. Instead, we must make use of the fact that quasienergy is small, which allows us to simplify the quartic Eq. (7) to

$$\chi^2 + \frac{i}{\tau}\chi - \frac{\delta_0^2\delta^2}{\Omega_R^2} = 0. \quad (18)$$

The bifurcation of the lifetimes is revealed in the imaginary parts of the quasienergies, which are given by

$$\chi_{\pm} = -\frac{i}{2\tau} \left[1 \pm \sqrt{1 - \frac{4\delta_0^2\delta^2\tau^2}{\Omega_R^2}} \right]; \quad (19)$$

see Fig. 2. For large Ω_R , solution $\chi_+ \approx -i/\tau$ corresponds to the S mode, while the solution $\chi_- \approx -i\delta_0^2\delta^2\tau/\Omega_R^2$ evolves into a long-living mode $\frac{1}{\sqrt{2}}(T_+ - T_-)$. In other words, strong ac drive induces a third long-living mode, which decouples from S and therefore cannot recombine. At the same time, the decoupling of S from all other triplet states makes its lifetime two times shorter than in the absence of drive. Note that there is a full formal correspondence between the solutions χ_+, χ_- and the superradiant and subradiant modes in the Dicke effect.¹⁸ On the physical level, in the Dicke effect, the subradiant mode acquires a long lifetime due to weak overlap with a photon field, while the long lifetime of the mode $\frac{1}{\sqrt{2}}(T_+ - T_-)$ is due to weak overlap with the recombining state S . With trapping by the subradiant mode incorporated, the correction to current takes the form

$$\frac{\delta I(\Omega_R)}{I(0)} = -\frac{\Omega_R^2}{(\delta_0^2\delta^2\tau\tau_D + \Omega_R^2)}. \quad (20)$$

It can be seen that the denominator in Eq. (20) defines a narrow domain $\delta_0 \sim \delta \sim \Omega_R^{1/2}/(\tau\tau_D)^{1/4}$, which yields the major contribution to $\langle \delta I(\Omega_R) \rangle$. Physically, this corresponds to configurations of the hyperfine fields in which *both* pair-partners are on-resonance. This again leads to the linear correction to $\langle \delta I(\Omega_R) \rangle$, which can be rewritten in dimensionless

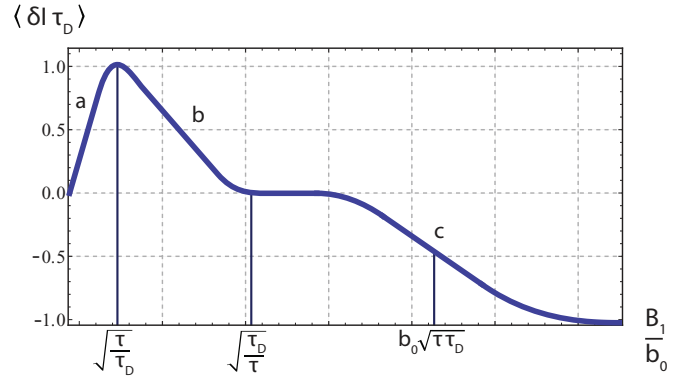


FIG. 4. (Color online) Schematic dependence of the radiation-induced correction to the current on the amplitude of the ac drive. Three prominent domains (a), (b), and (c) are described by Eqs. (14), (20), and (21), respectively.

units as

$$\frac{\langle \delta I(\Omega_R) \rangle}{I(0)} = -\frac{\Omega_R}{\pi b_0^2 \sqrt{\tau\tau_D}} \int dx \int dy \frac{1}{x^2 y^2 + 1}. \quad (21)$$

The double integral in Eq. (21) diverges, but only logarithmically, as $\ln[b_0^2(\tau\tau_D)^{1/2}/\Omega_R]$. In performing the averaging Eq. (21), we again replaced the distribution functions of δ, δ_0 by $\frac{1}{\sqrt{\pi}b_0}$. This replacement is justified provided the characteristic δ, δ_0 are much smaller than b_0 . The latter condition is equivalent to the condition that the argument of the logarithm is big. We should also check the validity of the expansion of the square root in Eq. (19). For characteristic δ, δ_0 the combination $\delta^2\delta_0^2\tau^2/\Omega_R^2$ is $\sim \tau/\tau_D \ll 1$; i.e., the expansion is valid. Overall dependence of $\langle \delta I \rangle$ on Ω_R exhibiting three prominent domains, Eqs. (14), (16), and (21), is sketched in Fig. 4.

VII. DISCUSSION

The prime experimental finding reported in Ref. 17, which motivated the present paper, is that the current blocking responsible for the OMAR effect⁸ is effectively lifted under magnetic-resonance conditions. We demonstrated that this lifting is a natural consequence of developing of the Rabi oscillations in one of the spin-pair partners. It is also known^{19–21} that Rabi oscillations in organic semiconductors, detected by pulsed magnetic resonance techniques, are dominated by pairs with one partner is on-resonance as well. The reason why both effects are due to the same sparse objects is that these objects are more responsive to the ac drive than nonresonant pairs. At the same time, the phase volume of such pairs is linear in Ω_R . Unfortunately, in the device design in Ref. 17, the magnitude of ac drive directly in the sample could not be measured. This precludes more quantitative comparison of our predictions with the experimental results. We hope that this comparison will be possible in the future as the experimental technique, used in Ref. 17, matures.

Besides the physical picture in the weak-driving domain, we also predict that the overall evolution of current with increasing B_1 is much more complex and involves a maximum followed by a drop and subsequent saturation; see Fig. 4. Note that strong deviation from linear dependence of δI sets in already at weak

driving fields, $B_1 \lesssim b_0$. The nonmonotonic behavior of current with ac drive is very unusual; its experimental verification would be a crucial test of radiation-induced trapping, which we predict.

Throughout the paper we assumed that the driving frequency exactly matches the Zeeman splitting γB_0 . In fact, in Ref. 17, the sensitivity of OMAR to the ac drive extended over a sizable interval of applied dc fields centered at B_0 . It is straightforward to generalize our consideration to a finite detuning $\Delta = \gamma B_0 - \omega_0$. Detuning enters the theory as a shift of the center of the Gaussian distribution of parameter δ from $\delta = 0$ to $\delta = \Delta$. Below we simply list the changes in the correction δI caused by strong detuning $\Delta \gg \gamma b_0$. These changes are different in different domains of the driving field shown in Fig. 4. For weak driving, the correction δI is given by

$$\frac{\delta I(\Omega_R)}{I(0)} = \frac{\Omega_R^2 b_0^2 \tau_D}{8\Delta^4 \tau}. \quad (22)$$

It emerges upon neglecting the Ω_R^2 term in the denominator of Eq. (13) and applies in the domain $\Omega_R \lesssim \Delta$ if Δ exceeds not only b_0 but also $b_0 \sqrt{\frac{\tau_D}{\tau}}$. Then, unlike Fig. 4, the change $\frac{\delta I}{I(0)}$

does not reach one. The maximal change is $\sim b_0^2 \tau_D / \Delta^2 \tau \ll 1$. Interestingly, the domain (c) in Fig. 4 is affected much weaker by the detuning, Δ . Instead of Eq. (21), we have

$$\frac{\delta I(\Omega_R)}{I(0)} = -\frac{\Omega_R}{\Delta b_0 \sqrt{\pi \tau \tau_D}}; \quad (23)$$

i.e., the linearity in Ω_R persists while the slope is suppressed by Δ/b_0 .

In conclusion, we note that one of our main findings, radiation-induced Dicke physics, goes way beyond the spin-dependent processes in organics. Previously the Dicke physics implied that one of the compound excited states of the system is orthogonal to the ground state, and hence the radiative decay is slow. We found that this orthogonalization of one of the excited states emerges in the “rotating frame” under strong enough ac drive and inhibits nonradiative recombination.

ACKNOWLEDGMENTS

We are grateful to W. Baker and C. Boehme for piquing our interest in the subject. This work was supported by the NSF through Grant No. MRSEC DMR-1121252.

¹V. Dediu, M. Murgia, F. C. Matocotta, C. Taliani, and S. Barbanera, *Solid State Commun.* **122**, 181 (2002).

²Z. H. Xiong, D. Wu, Z. Vally Vardeny, and J. Shi, *Nature (London)* **427**, 821 (2004).

³T. L. Francis, Ö. Mermer, G. Veeraraghavan, and M. Wohlgenannt, *New J. Phys.* **6**, 185 (2004).

⁴Ö. Mermer, G. Veeraraghavan, T. L. Francis, Y. Sheng, D. T. Nguyen, M. Wohlgenannt, A. Köhler, M. K. Al-Suti, and M. S. Khan, *Phys. Rev. B* **72**, 205202 (2005).

⁵Y. Sheng, D. T. Nguyen, G. Veeraraghavan, Ö. Mermer, M. Wohlgenannt, S. Qiu, and U. Scherf, *Phys. Rev. B* **74**, 045213 (2006).

⁶V. N. Prigodin, J. D. Bergeson, D. M. Lincoln, and A. J. Epstein, *Synth. Met.* **156**, 757 (2006).

⁷P. Desai, P. Shakya, T. Kreouzis, and W. P. Gillin, *Phys. Rev. B* **76**, 235202 (2007).

⁸P. A. Bobbert, T. D. Nguyen, F. W. A. van Oost, B. Koopmans, and M. Wohlgenannt, *Phys. Rev. Lett.* **99**, 216801 (2007).

⁹A. J. Schellekens, W. Wagemans, S. P. Kersten, P. A. Bobbert, and B. Koopmans, *Phys. Rev. B* **84**, 075204 (2011).

¹⁰B. Hu and Y. Wu, *Nat. Mater.* **6**, 985 (2007).

¹¹F. J. Wang, H. Bässler, and Z. Vally Vardeny, *Phys. Rev. Lett.* **101**, 236805 (2008).

¹²F. L. Bloom, W. Wagemans, M. Kemerink, and B. Koopmans, *Phys. Rev. Lett.* **99**, 257201 (2007).

¹³T. D. Nguyen, G. Hukic-Markosian, F. Wang, L. Wojcik, X.-G. Li, E. Ehrenfreund, and Z. V. Vardeny, *Nat. Mater.* **9**, 345 (2010).

¹⁴N. J. Harmon and M. E. Flatté, *Phys. Rev. Lett.* **108**, 186602 (2012); *Phys. Rev. B* **85**, 075204 (2012); **85**, 245213 (2012).

¹⁵R. C. Roundy and M. E. Raikh, *Phys. Rev. B* **87**, 195206 (2013); R. C. Roundy, Z. V. Vardeny, and M. E. Raikh, *ibid.* **88**, 075207 (2013).

¹⁶F. Wang, F. Macià, M. Wohlgenannt, A. D. Kent, and M. E. Flatté, *Phys. Rev. X* **2**, 021013 (2012); N. J. Harmon, F. Macià, F. Wang, M. Wohlgenannt, A. D. Kent, and M. E. Flatté, *Phys. Rev. B* **87**, 121203 (2013).

¹⁷W. J. Baker, K. Ambal, D. P. Waters, R. Baarda, H. Morishita, K. van Schooten, D. R. McCamey, J. M. Lupton, and C. Boehme, *Nature Commun.* **3**, 898 (2012).

¹⁸R. H. Dicke, *Phys. Rev.* **93**, 99 (1954).

¹⁹C. Boehme and K. Lips, *Phys. Rev. B* **68**, 245105 (2003).

²⁰D. R. McCamey, K. J. van Schooten, W. J. Baker, S.-Y. Lee, S.-Y. Paik, J. M. Lupton, and C. Boehme, *Phys. Rev. Lett.* **104**, 017601 (2010).

²¹R. Glenn, W. J. Baker, C. Boehme, and M. E. Raikh, *Phys. Rev. B* **87**, 155208 (2013).